

Influence of Microstructure on the Superconductivity of a Dilute Ti-Mo Alloy

E. W. Collings and J. C. Ho

Metal Science Group, Columbus Laboratories, Battelle Memorial Institute, Columbus, Ohio 43201

(Received 4 March 1969; revised manuscript received 8 July 1969)

Low-temperature specific-heat studies have shown that the superconducting transitions of thermally and mechanically induced martensitic structures, in quenched Ti-Mo ($4\frac{1}{2}$ at. %), occur in the range 2.5–3.2°K, compared to an estimated 0.5°K for the undistorted material. It is concluded that these thermal and deformation martensites are examples of structures in which “soft-phonon” modes are operative to increase T_c above what would be expected for unfaulted lattices of similar compositions.

INTRODUCTION

As Mo is added to Ti, the structure of solid-solution alloys after quenching from 1300°C [at which temperature they are all bcc (β)] is practically 100% hexagonal thermal martensite (α') up to $4\frac{1}{2}$ -at. % Mo; and retained β for concentrations higher than about 15-at. % Mo. In the composition range $4\frac{1}{2}$ -at. % Mo to 10-at. % Mo, electron microscope observations demonstrated the presence of a submicroscopic ($\sim 200 \text{ \AA}$) precipitate of

hexagonal structure (ω -phase) within the β matrix. From the abundance of ω phase seen in Ti-Mo (10 at. %), it is estimated that it will still occur in quenched alloys of up to about 15-at. % Mo. The concentration ranges of the various quenched structures [α' , ($\beta + \omega$) and β] are indicated in the inset to Fig. 1. In the titanium-rich field, Ti-Mo may be regarded as a prototype for alloys of the type $T-M$, where T represents either Ti, Zr, or Hf and M represents almost any other transition metal. Superconducting transition temperatures

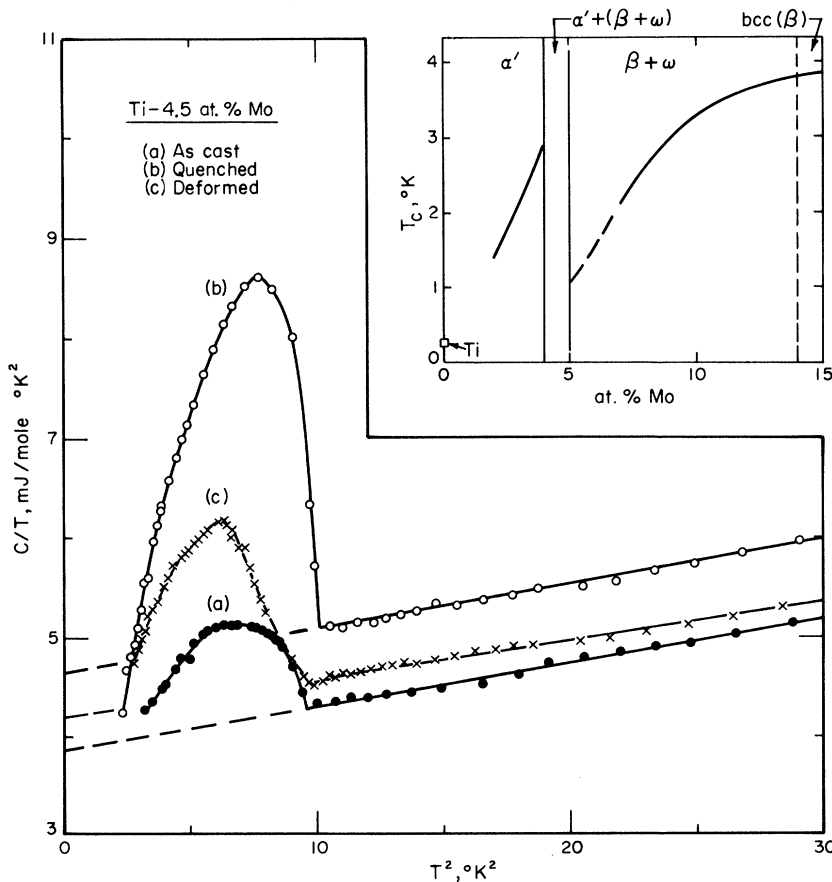


FIG. 1. Low-temperature specific-heat results for Ti-Mo ($4\frac{1}{2}$ at. %) in the conditions: quenched (Q), as-cast (C), and deformed from the as-cast condition (C+D). Inset shows the variation of superconducting transition temperature T_c with composition; the various microstructural regions are also indicated – after data by the present authors (Refs. 17 and 18).

(T_c) of dilute T - M alloys have been studied over a considerable period of time by many workers,¹⁻¹⁶ as indicated by Table I. By using low-temperature calorimetry (1.5–6°K) on a wide range of Ti-Mo alloys, the present authors¹⁷ have confirmed that T_c increases rapidly with solute concentration in the α' region. In α' Ti-Mo, T_c increased, at about the rate 1 deg / (at. % Mo), up to a value of $(2.9 \pm 0.2)^\circ\text{K}$ at 4-at. % Mo. We have also shown¹⁷ that T_c can be regarded as being anomalously "high" throughout the α' region, compared to what would be expected for nonmartensitic alloys with the same average electronic specific-heat coefficient γ . Proceeding to the bcc-based alloys, in quenched Ti-Mo (5 at. %) which marks the beginning of the $(\beta + \omega)$ field, T_c was immeasurably low in our calorimeter and therefore less than 1.5°K . The inset to Fig. 1 shows how the rapid increase in T_c with Mo concentration terminates abruptly at the end of the α' field, to increase again with concentration in the $(\beta + \omega)$ region. Superconductivity in the $(\beta + \omega)$ region of Ti-Mo alloys has also been discussed recently by the present authors.¹⁸ Therefore, since Ti-Mo ($4\frac{1}{2}$ at. %) was of critical composition, being at the boundary of the α' and $(\beta + \omega)$ fields, it was chosen for the following investigation; the purpose of which was to determine whether T_c was a function of structural transformation, at constant composition, from $(\beta + \omega)$ to (i) thermal martensite or (ii) deformation martensite.

COMPOSITIONS AND STRUCTURES

Optical metallography (Fig. 2) shows the struc-

TABLE I. Studies of T_c in dilute Ti- M and Zr- M binary transition-metal alloys.

Alloy or alloy system	Year	Ref.
Zr-Rh, Os	1957	1
Ti-Cr, Mn, Fe, Co	1959	2
Ti-Ru, Rh	1959	2
Ti-Mo	1961	3
Ti-V, Nb	1961	4
Ti-Nb	1961	5
Ti-Fe, Ru	1963	6
Ti-Rh, Zr-Rh	1963	7
Ti-Fe, Ru	1963	8
Zr-Co, Rh	1963	8
Ti-Mn	1963	9
Ti-V, Nb	1964	10
Ti-Co, Rh, Ir	1964	11
Zr-Co, Rh, Ir	1964	11
Ti-V, Nb, Mo	1964	12
Zr-Nb, Mo, Ru, Re	1965	13
Zr-Rh	1965	14
Zr-Nb	1966	15
Zr-Nb	1968	16

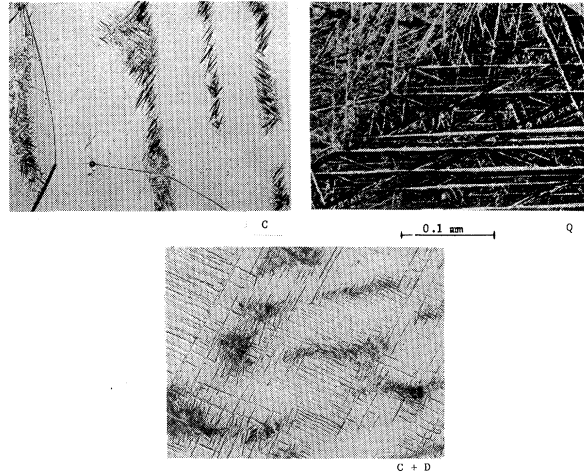


FIG. 2. Optical photomicrographs of Ti-Mo ($4\frac{1}{2}$ at. %) alloys. C: as-cast; martensitic transformation has occurred in small patches. Q: quenched; dense martensitic structure. C+D: specimen C after being deformed by compression.

ture of quenched Ti-Mo ($4\frac{1}{2}$ at. %)(henceforth Q) to be almost completely α' ; while in cast Ti-Mo ($4\frac{1}{2}$ at. %)(henceforth C) the α' was present only in small evenly spaced patches. The relative heights of the superconducting specific-heat anomalies in C and Q, respectively, (Fig. 1) reflected these observed relative abundances of α' . Clearly in C, which contained α' and $(\beta + \omega)$, the α' started to become superconducting at 3.1°K , while the $(\beta + \omega)$ matrix remained normal. Before proceeding further it was necessary to determine the Mo concentrations in the α' and $(\beta + \omega)$ regions of C with a view to determining whether a significant compositional difference existed between them. Electron-beam microprobe analysis was therefore carried out on C, together with quenched Ti-Mo ($4, 4\frac{1}{2}$, and 5 at. %) as calibrating specimens. The results of these measurements are summarized in Table II.

RESULTS

Thermal Martensite

The results of the low-temperature specific-heat measurements are plotted in their usual format in Fig. 1 [C/T versus T^2 , where C is the specific heat (mJ/mole deg), and T is the absolute temperature]. The intercept is the electronic specific-heat coefficient,¹⁹ γ which is approximately proportional to $n(E_F)$; the slope of the linear portion is a function of the Debye temperature Θ_D ; and the anomaly is due to the superconducting transition. The resulting data are summarized in Table III. By interpolation from measured da-

TABLE II. Microprobe analyses of dilute Ti-Mo alloys.

Nominal Mo concentration (at. %)	Heat treatment ^a and structure ^b	Chemical analysis (± 0.1 at. %)	Microprobe count-rate (counts/10 sec, \pm rms dev.)	Composition from microprobe analysis (at. %)
4	Q α'	3.9 ₄	327 \pm 3	
4 $\frac{1}{2}$	Q α'	4.5 ₁	376 \pm 13	
5	Q $\beta + \omega$	5.0 ₀	433 \pm 8	
4 $\frac{1}{2}$	C α'		368 \pm 6	4.3 ₈ \pm 0.0 ₈
	$\beta + \omega$		379 \pm 12	4.5 ₀ \pm 0.1 ₅

^aQ, 8 h at 1300 °C, quenched into iced brine; C, as cast [i.e., ($\beta + \omega$) with patches of α'].

^b α' - thermal martensite; ($\beta + \omega$) - bcc with precipitated ω phase.

ta¹⁸ relating to higher concentration Ti-Mo alloys (7, 8 $\frac{1}{2}$, 10, 15, 20, 25, and 40 at.%) and pure Ti, plotted in the format T_c/Θ_D versus $(0.212\gamma)^{-1}$,²⁰ T_c for undistorted Ti-Mo (4 $\frac{1}{2}$ at.%)_($\beta + \omega$) was estimated to be 0.5 °K. In contrast, for the α' component of C, Fig. 1 shows superconductivity to commence at 3.1 °K. The first experimental result is then obtained with the aid of Table II. A comparison of the data underlined shows that the Mo concentration in Q ($\sim 100\%$ α') is the same, within error, as that of the matrix ($\beta + \omega$) of C. It therefore follows that at constant composition, transformation of a structure from ($\beta + \omega$) to α' raises the superconducting transition threshold of Ti-Mo (4 $\frac{1}{2}$ at.%) from 0.5 to 3.2 °K.

Deformation Martensite

Referring again to Table II, it is seen that for specimen C itself the composition of the matrix ($\beta + \omega$) and the patches of α' in it were also equal within experimental error. That is to say, the composition of C was (a) uniform and (b) equal to that of Q. This fact raised a question as to the cause of the observed structural differences between C and Q (Fig. 2). It was thought that the

TABLE III. Summary of low-temperature specific-heat data for three specimens of Ti-Mo (4 $\frac{1}{2}$ at. %). [$C/T = \gamma + \beta T^2$, where γ , the electronic specific-heat coefficient, is proportional to $n(E_F)$, the Fermi density of states; and β yields Θ_D , the Debye temperature].

	C + D		
	Q (Quenched)	C (As-cast)	(Specimen C after deformation)
γ (mJ/mole deg ²)	4.65	3.85	4.20
Θ_D (°K)	350	350	365
T_c (°K) ^a	2.80 - 3.20	2.65 - 3.10	2.50 - 3.10

^aTemperatures noted are the peak and onset, respectively, of the calorimetric specific-heat anomaly.

almost complete transformation to martensite in Q (as compared to C) was partly a result of mechanical deformation accompanying the rapid ice-brine quench. If this were so, it was postulated that a comparable effect should be obtained upon mechanically deforming C isothermally at room temperature. Indeed, after subjecting C to compression to the point of fracture²¹ a repetition of the specific-heat experiment (C+D in Fig. 1) revealed that an increased proportion of the material was able to undergo a superconducting transition in the range 2.5-3.1 °K. In addition, the volume fraction of martensite was increased by the compression. Figure 2 (C+D) shows the deformation-induced martensite extending from the initial patches out into the matrix.

To summarize, it is concluded from these experiments that structural transformation of a ($\beta + \omega$) Ti-Mo (4 $\frac{1}{2}$ at.%) alloy to either thermal (α') or deformation martensite, raises the superconducting transition temperature from 0.5 °K to the vicinity of 2.5 to 3.2 °K.

DISCUSSION

Superconductivity in Disordered Structures

Superconductivity in various kinds of disordered structures has been considered by Garland *et al.*²² [(a) homogeneous amorphous films, (b) amorphous metallic granules, and (c) microcrystalline films], and by Strongin *et al.*²³ (layered metallic films), against a theoretical background provided by McMillan.²⁴ In such distorted structures the observed enhancements of T_c have been regarded as being due to increased superconducting electron coupling through reductions of the mean square phonon frequency (ω^2) arising from atoms occupying sites of reduced symmetry. According to McMillan²⁴ the superconducting transition temperature may be expressed as

$$T_c = \frac{\Theta_D}{1.45} \exp\left(-\frac{1.04(1+\lambda)}{\lambda - \mu^*(1+0.62\lambda)}\right), \quad (1)$$

where λ is the electron-phonon coupling constant, and μ^* is the Coulomb "pseudopotential." When coupling is weak, as defined by $\lambda \ll 1$, Eq. (1) reduces to the BCS-Morel²⁰ relationship

$$T_c \propto \Theta_D \exp[-1/n(E_F)V], \quad (2)$$

but with an interaction strength $(\lambda - \mu^*)$ taking the place of the $n(E_F)V$, where V is the pairing potential.

The Coulomb pseudopotential μ^* may under favorable conditions be obtained from the isotope shift δ , T_c , and Θ_D by means of

$$\mu^* = (1 - 2\delta)^{1/2} / \ln(\Theta_D/1.45T_c), \quad (3)$$

enabling an empirical value of λ to be calculated from

$$\lambda = \frac{\mu^* \ln(\Theta_D/1.45T_c) + 1.04}{(1 - 0.62\mu^*) \ln(\Theta_D/1.45T_c) - 1.04}, \quad (4)$$

which is a rearrangement of Eq. (1).

According to our observations, the thermal and deformation-induced martensites are further examples of structures which are favorable to the existence of low-frequency localized vibrations of relatively large amplitude or "soft-phonon modes." The effect of such "lattice softness" is to increase T_c above what would be expected for an unfaulted structure [e. g., $(\beta + \omega)$] of similar composition.

Martensitic Structures

It is well known that martensitic transformation takes place by a process of lattice shearing. The resulting structure generally appears as platelets formed by two successive shear displacements. This mechanism of transformation is subject to frequent departures from coherent atomic motion. As a result the martensitic structure is so detailed that it can be properly studied only in the electron microscope. Such observations show the platelets to be heavily faulted, within themselves, and separated one from the other by regions of untransformed matrix. Because of this, both spontaneously transformed structures (thermal martensite), and structures resulting from transformation under stress (deformation martensite), must contain relatively large proportions of atoms occupying sites of reduced symmetry. These conditions are favorable for the existence of high densities of localized vibrational states.

Thermal Martensite

As shown in Table III, the measured average electronic specific-heat coefficient γ is equal to 3.85 in C [which is mostly $(\beta + \omega)$] and to 4.65 in Q (which is mostly α'). The expected T_c ratio, on the basis of Eq. (2) is therefore 2.2. But the

experiments show that T_c increases by a factor $3.2/0.5 \approx 6$. It follows that the transition temperature must also be sensitive to structure presumably through its influence on the phonon frequencies. It is therefore appropriate to apply McMillan's treatment, as outlined below.

In Eq. (3), δ , which does not seem to have been determined for Ti, will be assumed to be equal to that for Zr, i. e., zero.²⁴ Using the present calorimetric data for Ti-Mo ($4\frac{1}{2}$ at. %) _{$(\beta + \omega)$} , that equation then gives $\mu^* = 0.16$. Equation (4) may then be solved yielding $\lambda = 0.5_0$ for Ti-Mo ($4\frac{1}{2}$ at. %) _{$(\beta + \omega)$} .

McMillan has discussed how a maximal value of T_c may be obtained for a given "class of materials" by optimizing the average phonon frequency. These calculations have resulted in a graph of $T_c/T_{c_{\max}}$ (i. e., reciprocal of the maximal T_c enhancement factor) versus λ , in case $\mu^* = 0.13$ which is not significantly different from our $\mu^* = 0.16$. An uncritical application of this plot for $\lambda = 0.5$, which is probably near to being a lower limit for the strict validity of the McMillan method, yields $T_{c_{\max}}/T_c = 9$. The results of the present experiments are

$$T_{c_{\alpha'}}/T_{c_{(\beta + \omega)}} = 3.2/0.5 = 6.$$

But the same experiments also yielded $\gamma_{\alpha'}/\gamma_{(\beta + \omega)} = 4.65/3.85$ which leads to a T_c ratio of 2.2 according to the BCS [Eq. (2)] relationship. We therefore assess the phonon-induced enhancement factor to be about 3.

Deformation Martensite

Figure 1 shows that when C is deformed, although the material which transforms superconductively increases (curve $C + D$), the specific-heat anomaly is not magnified uniformly. Obviously in $C + D$ a range of T_c 's exists, the highest of which is 3.1 °K. A comparison of C and $C + D$ in Fig. 1 suggests that the deformation martensite tends to transform at a lower temperature than does thermal martensite. This is demonstrated more clearly by Fig. 3 which is a plot of C_D/T versus T^2 , where $C_D (\equiv C_{C+D} - C_C)$ represents the increase in specific heat brought about by the deformation. Three features are noticeable: (a) the expected small positive γ_D , (b) an increase in C_D , representing the onset of superconductivity in deformation martensite, commencing at about 2.8 °K, (c) finally, a "negative-going" segment of the curve indicating that a part of the material, which could become superconducting near 3.1 °K prior to deformation, transforms at some lower temperature after deformation.

The thermal-martensitic phase α' formed on quenching Ti-Mo alloys is well known to have a

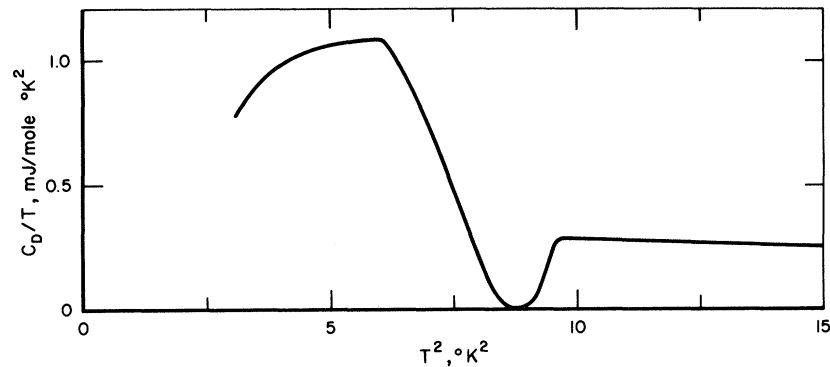


FIG. 3. Difference between the low-temperature specific heats of $(C+D)$ and C plotted in the format C/T versus T^2 . The positive-going portion is a result of superconducting transitions in the deformation martensite; the negative-going section is interpreted as being due to suppression of superconductivity in those regions of α' situated in proximity to the deformation martensite.

hexagonal structure. On the other hand, recent studies by Blackburn and Williams²⁵ on deformation-induced martensite in Ti-Mo have revealed a bcc or bc-tetragonal structure. It is therefore reasonable that the two forms of martensite should have different superconducting transition temperatures. Figure 2 shows the regions of thermal and deformation martensites to overlap each other. Thus, the partial suppression of T_c , as evidenced by the negative-going segment in Fig. 3, could reasonably be due to a proximity effect operating between some of the deformation martensite ($T_c \cong 2.5$ to 2.8°K) and those parts of the thermal martensite ($T_{c_{\text{max}}} = 3.1^\circ\text{K}$) adjacent to it.

CONCLUSION

As a result of low-temperature calorimetry, if the superconducting transition temperatures of a series of Ti-Mo alloys (rapidly quenched from 1300°C) are compared with the corresponding γ 's through a BCS-type relationship, they appear to be anomalously high for alloys in the concentration range $0 < \text{at. \% Mo} < 4\frac{1}{2}$. In just this range the microstructure is thermal martensitic α' , as distinct from the bcc (β) structure of higher-concentration alloys (although an ω -phase precipitate is present in the " β " alloys of up to 15-at. % Mo). It was, therefore, of interest to observe the structural dependence of T_c at constant composition. For this purpose an alloy of $4\frac{1}{2}$ -at. % Mo was chosen since this was on the borderline between the α' and $(\beta + \omega)$ phase fields. In the as-cast condition Ti-Mo ($4\frac{1}{2}$ at. %) contains little α' , but a high abundance of it can be induced by quenching from elevated temperatures. Furthermore, in this alloy, as in those of compositions of up to about 7-at. % Mo, martensite can be induced by deformation at room temperature. It was deduced, from the calorimetric data for higher concentration Ti-Mo alloys, that T_c [Ti-Mo ($4\frac{1}{2}$ at. %) $_{(\beta+\omega)}$] = 0.5°K . The threshold T_c for α' in the same alloy was 3.2°K , while that for the deformation martensite was about 2.8°K .

The same experiments also showed that $\gamma_{\alpha'}/\gamma_{(\beta+\omega)} \cong 4.65/3.85$. We therefore conclude that the martensitic structures were responsible for significant enhancements (factor of 3) of the superconducting transition temperatures over what would be expected (factor of 2.2) from the BCS relationship [Eq. (2)] and the above γ ratio.

It has previously been suggested, particularly with reference to V_3Si , that a relationship exists between a lattice instability which results eventually in a low-temperature martensitic transformation at T_m , and the onset of superconductivity at $T_c < T_m$. In V_3Si , for which $T_c = 17^\circ\text{K}$, Batterman and Barrett²⁶ first showed by x-ray measurements the occurrence of a martensitic transformation at about 21°K . This was later confirmed by specific-heat and resistivity measurements²⁷ and acoustic studies.²⁸ The sound velocity and attenuation work²⁸ together with recent Young's modulus studies²⁹ now make it clear that in V_3Si a large low-temperature lattice instability, for shear waves propagating along the $[1\bar{1}0]$ polarization, leads to a martensitic-type transformation; and it has been pointed out²⁹ that this instability becomes completely arrested at a few degrees below T_c . In contrast, the V_3Ir lattice remains stable and also non-superconducting down to 0.3°K . Consequently, considerable attention has been devoted to searching for a relationship between structural instabilities and the occurrence of superconductivity. A connection between these properties has been made through band-structure studies by Cohen *et al.*,³⁰ and by the Orsay group.³¹

In the alloy system considered here T_c and T_m are not in proximity. In fact T_m for Ti-Mo ($4\frac{1}{2}$ at. %), according to some authors,^{32,33} is about 500°C . We interpret our results as indicating that an enhanced T_c is a property of the distorted lattice itself; and that the observed threefold enhancement is consistent with McMillan's prescription. As mentioned above, enhanced T_c 's have been predicted or observed for (a) homogeneous amorphous films,

(b) amorphous metallic granules, (c) microcrystalline films, and (d) layered metallic films. We conclude that martensitic structures, whether induced thermally or mechanically, are further examples of configurations in which T_c is enhanced through a soft-phonon-mode type of mechanism.

ACKNOWLEDGMENTS

We wish to thank G. Waters and R. D. Smith for

specimen preparation and optical metallography and C. Martin for electron microscopy. We are also grateful to Dr. J. D. Boyd, Battelle; and Dr. J. Labbé and Dr. S. Barišić, Orsay, for helpful and stimulating discussions. The financial assistance of Battelle-Columbus Laboratories, and the U. S. Air Force Materials Laboratory, Wright-Patterson Air Force Base, Ohio [Contract No. AF 33(615)-3967] is also acknowledged.

¹B. T. Matthias, in *Progress in Low-Temperature Physics*, edited by C. J. Gorter (North-Holland, Amsterdam, 1957), Vol. 2, p. 139.

²B. Matthias, V. B. Compton, H. Suhl, and E. Corenzwit, *Phys. Rev.* **115**, 1597 (1959).

³R. D. Blaugher, B. S. Chandrasekhar, J. K. Hulm, E. Corenzwit, and B. T. Matthias, *J. Phys. Chem. Solids* **21**, 252 (1961).

⁴E. Bucher and J. Muller, *Helv. Phys. Acta* **34**, 410 (1961).

⁵J. K. Hulm and R. D. Blaugher, *Phys. Rev.* **123**, 1569 (1961).

⁶B. T. Matthias, in *Proceedings of the Eighth International Conference on Low-Temperature Physics*, edited by R. O. Davis (Butterworth, London, 1963), p. 135.

⁷Ch. J. Raub and C. A. Anderson, *Z. Physik* **175**, 105 (1963).

⁸B. T. Matthias, T. H. Geballe, and V. B. Compton, *Rev. Mod. Phys.* **35**, 1 (1963).

⁹R. L. Falge, *Phys. Rev. Letters* **11**, 248 (1963).

¹⁰F. Heiniger and J. Muller, *Phys. Rev.* **134**, A1407 (1964).

¹¹Ch. J. Raub and G. W. Hull, *Phys. Rev.* **133**, A932 (1964).

¹²E. Bucher, F. Heiniger, J. Muller, in *Proceedings of the Ninth International Conference on Low-Temperature Physics, Columbus, Ohio, 1964*, edited by J. G. Daunt (Plenum, New York, 1965), p. 482.

¹³J. O. Betterton and J. O. Scarbrough, ORNL Report No. 3870, 1965 (unpublished).

¹⁴S. T. Zegler, *J. Phys. Chem. Solids* **26**, 1347 (1965).

¹⁵R. F. Hehemann and S. T. Zegler, *Trans. AIME* **236**, 1594 (1966).

¹⁶J. M. Corsan, I. Williams, J. A. Catterall, and A. J. Cook, *J. Less Common Metals* **15**, 437 (1968).

¹⁷E. W. Collings and J. C. Ho, *Phys. Letters* **29A**, 306

(1969).

¹⁸J. C. Ho and E. W. Collings, *Phys. Letters* **29A**, 206 (1969).

¹⁹For free electrons $0.212 |\gamma_0| = |n(E_F)|$, referring to a single spin direction, where $|\gamma| = \text{mJ/mole deg}^2$, and $[n(E_F)] = (\text{eV atom})^{-1}$.

²⁰The usefulness of such a plot, based on a BCS-Morel [J. Phys. Chem. Solids **10**, 277 (1959)] formula, $T_c = 0.85 \Theta_D \exp[-1/n(E_F) V]$, will be discussed elsewhere.

²¹The maximum load applied to a roughly cubical specimen of mass 20 g was about 59 000 lb.

²²J. W. Garland, K. M. Bennemann, and F. M. Mueller, *Phys. Rev. Letters* **21**, 1315 (1968).

²³M. Strongin, O. F. Kammerer, J. E. Crow, R. D. Parks, D. H. Douglass, Jr., and M. A. Jensen, *Phys. Rev. Letters* **21**, 1320 (1968).

²⁴W. L. McMillan, *Phys. Rev.* **167**, 331 (1968).

²⁵M. J. Blackman and J. C. Williams, *Trans. AIME* **242**, 2461 (1968).

²⁶B. W. Batterman and C. S. Barrett, *Phys. Rev. Letters* **13**, 390 (1964); also *Phys. Rev.* **145**, 296 (1966).

²⁷J. E. Kunzler, J. P. Maita, E. J. Ryder, H. J. Levinstein, and F. S. L. Hsu, *Bull. Am. Phys. Soc.* **10**, 319 (1965).

²⁸L. R. Testardi, T. B. Bateman, W. A. Reed, and V. G. Chirba, *Phys. Rev. Letters* **15**, 250 (1965).

²⁹T. R. Finlayson, E. R. Vance, and W. A. Rachinger, *Phys. Letters* **26A**, 474 (1968).

³⁰R. W. Cohen, G. D. Cody, and J. J. Halloran, *Phys. Rev. Letters* **19**, 840 (1967).

³¹J. Labbé, *Phys. Rev.* **172**, 451 (1968).

³²P. Duwez, *Trans. ASM* **45**, 936 (1953).

³³E. K. Molchanova, *Phase Diagrams of Titanium Alloys*, (Israel Program for Scientific Translations, Jerusalem, 1965), p. 29.

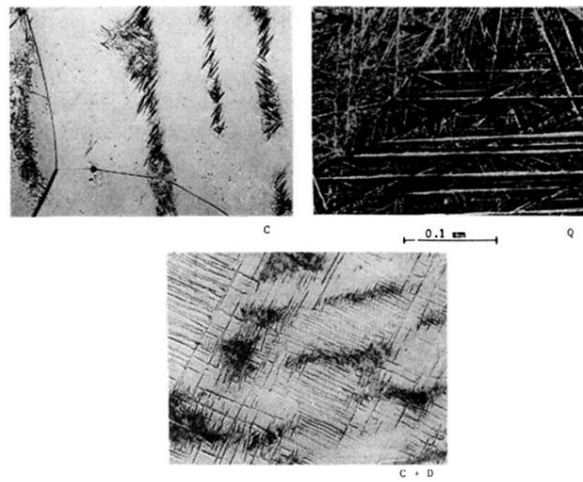


FIG. 2. Optical photomicrographs of Ti-Mo ($4\frac{1}{2}$ at. %) alloys. *C*: as-cast; martensitic transformation has occurred in small patches. *Q*: quenched; dense martensitic structure. *C+D*: specimen *C* after being deformed by compression.